USE OF IMPEDANCE SPECTROSCOPY TO STUDY THE INTEGRITY OF THE ALUMINIUM OXIDE FILMS IN MERCURY EMBRITTLED ALUMINIUM

R.E.Clegg[1], A.Srivastava[2], Amoghavarsha M.[3]
[1]Process Engineering and Light Metals Centre, CQUniversity, Gladstone, [2]Department of Materials Science and Engineering, Stanford University, Stanford, CA, USA, [3]NITK, Srinivasnagar, Surathkal, Karnataka, India.

SUMMARY: Mercury embrittlement is a significant issue in the gas processing industry, where the precipitation of mercury from the gas stream in cryogenic heat exchangers can lead to embrittlement of the aluminium structure and it has been the cause of several significant failures. This paper studies the use of impedance spectroscopy to examine the interface between mercury droplets and 5083 aluminium. As-received, mechanically polished and artificially aged samples were examined using a two electrode mode with a zero bias. The Nyquist results indicated that as-received and polished and aged samples behaved as an R_s-C-R_p type circuit, indicating that the oxide film could be modelled as a capacitor and resistor in parallel. Using the dielectric constant of alumina, the capacitance results yielded oxide films of thickness between 2.2 and 50 nm, depending on the degree of aging of the sample. By gradually increasing the voltage amplitude, it was found that the interface broke down at a field strength of approximately 10MV/m, which is similar to the dielectric field strength of alumina. Immediately after polishing, however, no film was found and the interface appeared to be a simple short circuit. A series of bend tests coupled with the frequency response analyser were used to demonstrate that the film remained continuous beyond the point at which plastic deformation occurred and in many cases up until the point at which embrittlement occurred. These results have confirmed that the oxide film on aluminium can effectively separate mercury from the underlying aluminium alloy and that impedance spectroscopy is a useful tool for studying the stability of the interface.

Keywords: Mercury Embrittlement, gas processing, fracture, liquid metal induced embrittlement.

1. INTRODUCTION

Mercury embrittlement of aluminium cryogenic heat exchangers is an established problem and has been the cause of a number of failures in the natural gas processing industry [1-6]. Mercury is present in many sources of natural gas in varying quantities. In the process of compression and preliminary separation, gas is chilled and compressed until the heavier fractions of the gas are liquefied. During this process, it is possible for mercury to precipitate and accumulate in the cryogenic heat exchangers. Many cryogenic heat exchangers are made of 5083 aluminium and it is possible that liquid mercury can be present on the surface of these heat exchangers. Mercury is known to severely embrittle aluminium alloys and a number of failures have been recorded[3, 5-7].

It is possible that mercury may be present on the surface of structural components in gas processing equipment for a considerable length of time without causing failure. It has been postulated that the reason for this is that the oxide film on the aluminium provides a strong, impenetrable barrier to the mercury, effectively separating the mercury from the aluminium[3]. However, it is also known that under certain circumstances, this barrier breaks down and leads to embrittlement or oxidation of the aluminium. The nature of passive oxide films in aluminium has been studied for many years, particular concerning its formation in aqueous media[8-11], but the formation of passive oxide films in air has been less well examined[10]. In natural gas plants, the oxide films may be formed under a number of conditions. First, much of the equipment will have passive films formed during the manufacture of the plate and during subsequently exposure of the plate in the atmosphere. Once the plates are welded, the passive film around the weld will be influenced by the welding procedure and the conditions of welding. This is likely to lead to different behaviour around welds compared with parent plate. Finally, areas of the passive film may become damaged during the operation of the plant, possibly the result of solid

contaminants in the gas stream abrading the surface of the aluminium in service. Under these conditions, the films will reform in oxygen-poor low-temperature dry conditions. The reactions between the mercury droplets and oxide films formed under various conditions are poorly understood and if the formation of oxide films on the surface of aluminium heat exchangers is to provide a reliable and effective barrier to embrittlement, then a greater understanding of these reactions are necessary.

This paper presents a study of the aluminium-mercury interface using impedance spectroscopy using plate samples of Al 5083-H116/321, a commonly used alloy in heat exchanger construction. Although impedance spectroscopy has been used by some authors previously, it has had only limited success[12]. This is probably because high voltages used in previous experiments tended to lead to breakdown of the interface, as shown later in this paper. Impedance spectroscopy is used to measure the integrity of the film and to study the effects of some environmental parameters on the ability of the film to provide an effective barrier to the mercury. In this study, the interface can be described as an R-C-R type equivalent circuit similar in form to that shown in Figure 1. In Figure 1, the capacitor is represented as a constant phase element, as the CPE was shown to more accurately represent the experimental results. As described below the CPE can be converted to an effective capacitance component, C_{eff}. The capacitance component (C_{eff}) of the equivalent circuit will give an indication of the average film thickness through the following equation.

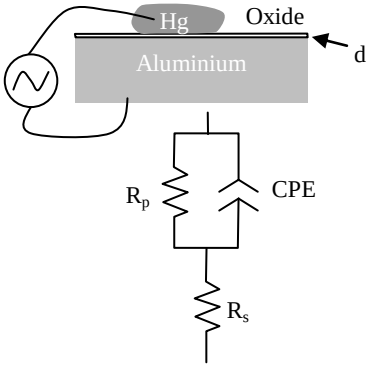

Figure 1 Electrical model for the interface incorporating a constant phase element, rather than a capacitance.

$$d = \frac{A\varepsilon\varepsilon_o}{C_{eff}} \quad (1)$$

where d is the film thickness (see Figure 1), A is the area of contact between the mercury and aluminium oxide film, ε_0 is the permittivity of a vacuum and ε is the relative dielectric constant of the material. In this technique, the complex impedance of a corrosion cell is measured over a range of frequencies. At each frequency, the complex impedance, Z, is determined.

$$Z = Z' + jZ'' \quad (2)$$

Where Z' is the real component and Z'' is the imaginary component of the complex impedance and Z' and Z'' are plotted on a Nyquist plot which can be used to check the effectiveness of models for the interface and reactions taking place.

1.1 Determination of effective capacitance and film thickness from constant phase element

The results have shown that in many instances, the impedance of the interface can be most effectively modelled using a constant phase element, rather than an ideal capacitor. A constant phase element (CPE) can be regarded as an imperfect capacitor. According to Hirschorn *et al.*[13], the electrical response of the circuit shown in Figure 1can be given by the following equation.

$$Z(\omega) = R_s + \frac{R_p}{1+(j\omega)^{\alpha}QR_p} \quad (3)$$

where $Z(\omega)$ is the complex impedance at a frequency of ω, Q and α are CPE parameters that are independent of frequency. α varies from 0 to 1, where 0 represents behaviour similar to a perfect resistor and 1 represents behaviour similar to a perfect capacitor. The interpretation of what a CPE means is still the subject of debate. In particular, whilst it is possible to calculate Q from impedance spectrum data, Q cannot be used alone as an effective capacitance, as it tends to underestimate the true thickness of the film. Several models have been used to try to convert the impedance data to an effective capacitance (C_{eff}) that can be used to determine film thickness.

The assumption used in this paper is that the nature of the film varies through the thickness and the film impedance can be modelled as a series of RCR circuits. In this case, the CPE behaviour of the film occurs predominantly when the films are thick or are formed in a moist atmosphere. It seems plausible, therefore, the films will vary structurally and electrically in the direction normal to the surface and so this model is used to determine the effective capacitance. From Hirschorn et al.[13], the effective capacitance can be given by the following equation.

$$C_{eff} = Q^{1/\alpha}.R_p^{\frac{(1-\alpha)}{\alpha}} \quad (4)$$

2. MATERIALS AND METHODS

Oxide file measurements were carried out using plate samples of Al 5083-H116/321 and extruded bar of aluminium 6061. In the first series of tests, the polished samples were prepared by grinding the surfaces with progressively finer metallographic grinding papers until the surface was ground with P600 grit paper. The surfaces were then mechanically polished with 6μm and 1μm metallographic diamond pastes. Aging of the surfaces was carried out in dry air. The dry air atmosphere was created by enclosing the samples in a box with silica gel desiccant. Aging was carried out for up to 2 months and at room temperature (23°C in an air-conditioned room).

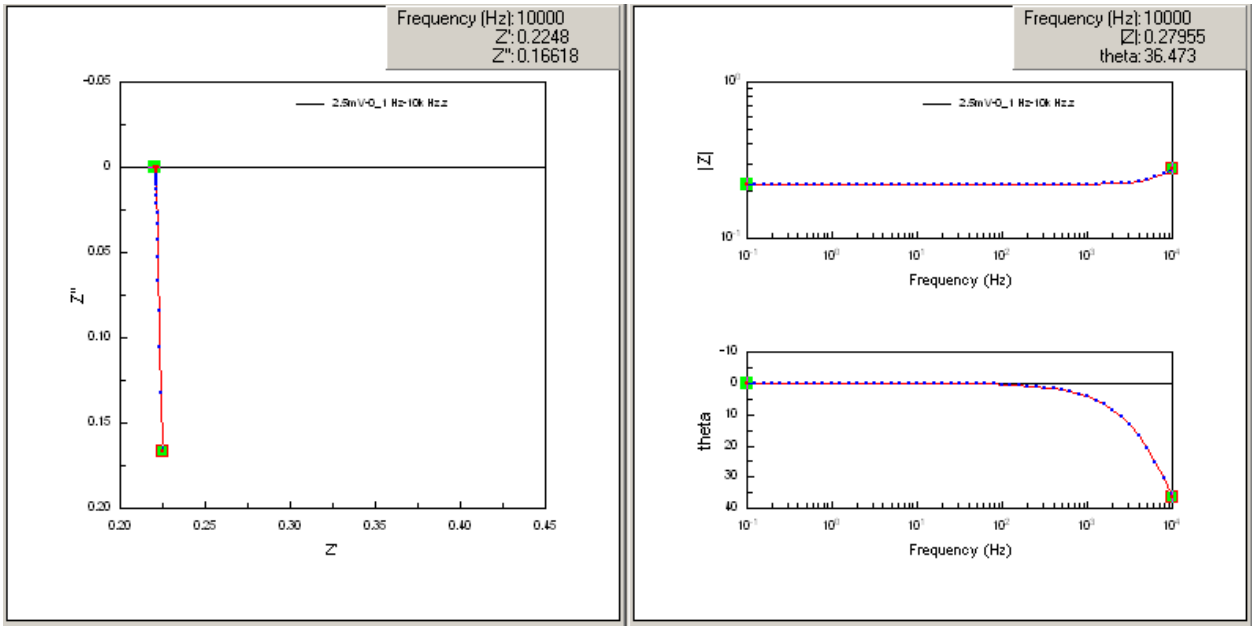

Figure 2 Typical Nyquist and Bode plots for a mercury droplet on polished aluminium moments after the aluminium was polished and exposed to laboratory air.

Representative surfaces were examined using an optical microscope and using a JEOL JSM 6360 LA scanning electron microscope, which allowed for EDS mapping and spot analysis of the surface. The microscope was used in secondary electron mode with an accelerating voltage of 15kV. Prior to testing, a mercury droplet was placed on the surface of the aluminium samples such that a contact area of approximately 5 mm diameter was maintained. Electrical contact was made on the aluminium via metallic clips and in the mercury through a 0.1mm diameter platinum wire. The impedance of the interface was measured using a Solartron 1260 in stand-alone mode and Zplot software. The equivalent circuits were calculated using Zview. Once testing was completed, the mercury droplet was weighed to an accuracy of 0.0001 g and the weight was related via a calibration curve to the area of contact between the mercury and aluminium. Most of the droplets used in these experiments were between 0.4 and 1.0 g in weight. All tests were carried out at room temperature in an air conditioned room (23°C).

A series of eight samples were tested under load by plastically deforming samples with mercury droplets on the surface. The surfaces were prepared by mechanically polishing and then aging overnight. The samples were 200 × 20 × 6 mm and were loaded in 3 point bending with the rollers separated by 150 mm (75 mm arm length). The load *vs* crosshead position was monitored and the impedance of the films was measured at intervals of 0.1 mm crosshead position. The point at which the short circuited through the film was noted.

3. RESULTS

3.1 Measurement of the oxide film characteristics

Measurement of the oxide film was carried out using the impedance spectroscopy techniques as described above. Initial studies were carried out on freshly polished surfaces. These were exposed to the laboratory atmosphere only for a few moments prior to testing. It is generally acknowledged that the oxide film on aluminium forms rapidly and within the first few moments of exposure to air. However, in the tests carried out here, the freshly formed oxide film could not be detected by impedance measurements. Figure 2 shows typical Nyquist and Bode plots for a sample of as-received and polished 5083 exposed to mercury moments after it was polished and exposed to laboratory atmospheric air. As can be seen, the sample exhibits characteristics of a short circuit, with little or no development of a capacitance layer. Under these circumstances, the film, if present, is acting purely as a resistor.

After a period of aging in laboratory air, the samples began to display characteristics of the formation of a capacitive film. Typical Nyquist and Bode plots for such a film is as shown in Figure 3. As can be seen from the figure, the Nyquist plot developed the characteristic semicircular shape that is typical of an R-C-R type equivalent circuit as shown in Figure 1. In this particular example the sample showed a change in behaviour at lower frequencies. In general, this tended to occur in cases where the mercury was present on the surface for only a relatively short period of time. It became apparent during the testing that interface between the mercury droplet and the aluminium was relatively instable initially and this could lead to relatively unpredictable behaviour during the impedance sweeps, particularly at the lower frequencies. The longer the droplet was left on the surface the more predictable the impedance sweep became. In the most stable cases, the Nyquist plots became quite clean semicircles.

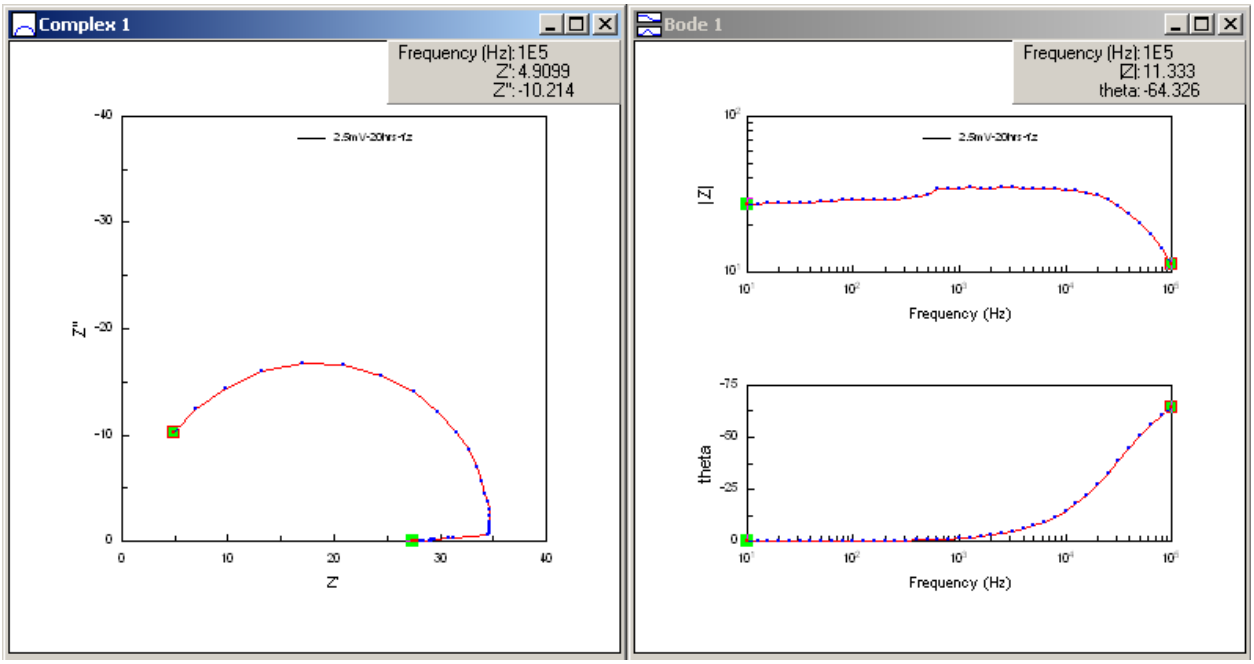

Figure 3 Typical Nyquist and Bode plots for an as-received and polished sample aged in laboratory air for 24 hrs prior to being exposed to a mercury droplet.

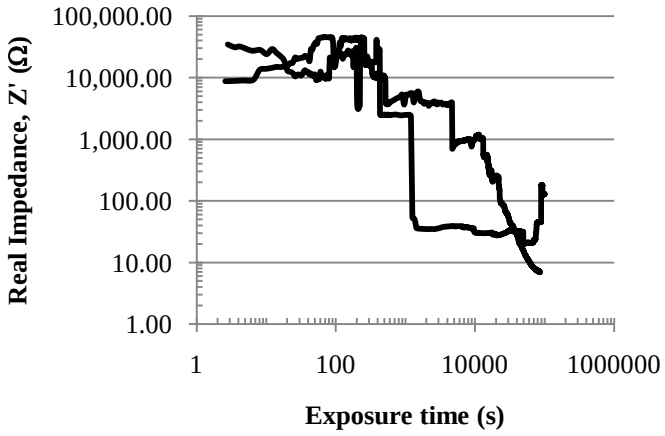

Figure 4 Effect of exposure time on the real impedance, Z', measured at 10 Hz for samples aged for 1600 hrs in dry air,

Another example of how the instability of the interface could be manifested is shown in, which shows the effect of time on the real impedance, Z'. The test was carried out by measuring the complex impedance of the mercury-aluminium interface at a frequency of 10 Hz and intervals of 2 s. Figure 4 and Figure 5 were for two samples of as-received 5083 that had been polished and aged in dry air for 1600 hrs prior to testing. As can be seen, the interface was quite unstable over the period of exposure and eventually developed a short circuit characteristic towards the end of the time period. The Nyquist plots of these two samples are interesting also and are shown in Figure 5. The Nyquist plot shows a curve that is characteristic of a circuit as shown in Figure 1 where only R_p changes with time. In fact the deduction that can be drawn from this Figure is that during the aging process, film capacitance (or constant phase element) does not change significantly, but that the changes in complex impedance are entirely due to the changes in the parallel resistance. The use of 10 Hz as a measuring frequency was initially because the first results obtained at this frequency showed small complex impedances relative to the real impedance and so it was reasonable to assume that the measurement at 10 Hz provided real impedances that were close to the $R_p + R_s$ value, where $R_s << R_p$. However, these later studies have shown that as R_p increases, the complex impedance becomes significant, leading to curves such as Figure 5. To verify this, Equation 3 was simulated using Matlab. In this simulation, only R_p was varied and the resulting curve was similar to that shown in Figure 5. Furthermore, a series of tests were carried out where the full frequency varying impedance sweep was carried out over

time and this verified that the film thickness as measured through the capacitance (or CPE) did not vary significantly with time but the parallel resistance could vary, depending on the way in which the sample was aged.

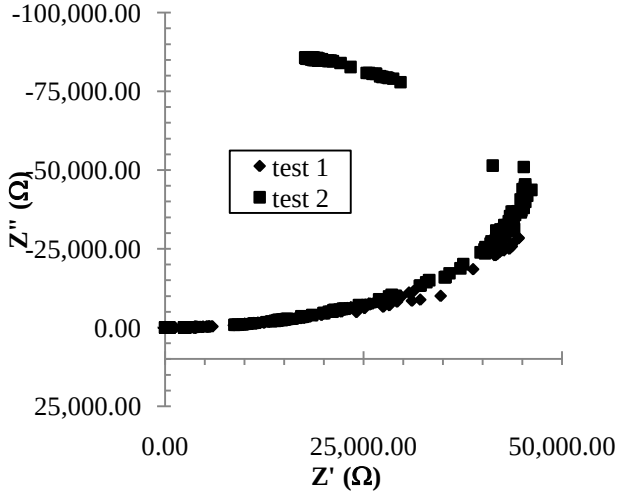

Figure 5 Nyquist plot of the time based data shown in Figure 4.

3.2 Oxide film breakdown

A series of tests were carried out to measure the effects of voltage amplitude on the impedance measurements. The tests were carried out on a variety of films with different thicknesses. The procedure of the tests was to carry out a series of full frequency varying sweeps at gradually increasing voltage amplitudes. Figure 6 shows an example of these sweeps with increasing voltage amplitude. In this set of experiments, the voltage amplitude of the impedance sweeps was increased from 20mV to 900 mV. The frequency range of these experiments was from 100kHz to 1Hz. As can be seen from Figure 6 a, initially the response was typical of the R-C-R circuit previously described although only a small portion of the semicircle on the Nyquist plot could be obtained in these tests. In other tests, where the oxide film was thinner the characteristic semicircle of the Nyquist plot was achieved. However, as can be seen in these tests, the impedance of the film was initially high. Under these conditions, the film thickness was measured at approximately 20 nm. As the voltage amplitude increased, the behaviour changed abruptly. As can be seen, at about 700mV, the Nyquist plot began to breakdown and it appeared that the parallel resistance of the film decreased significantly from approximately 2,000,000 Ω to 4000 Ω. At 800 mV, the impedance recovered slightly but then broke down again as the frequency decreased during the test. As the voltage amplitude was increased further to 900 mV, the film broke down completed and the film acted as a short circuit.

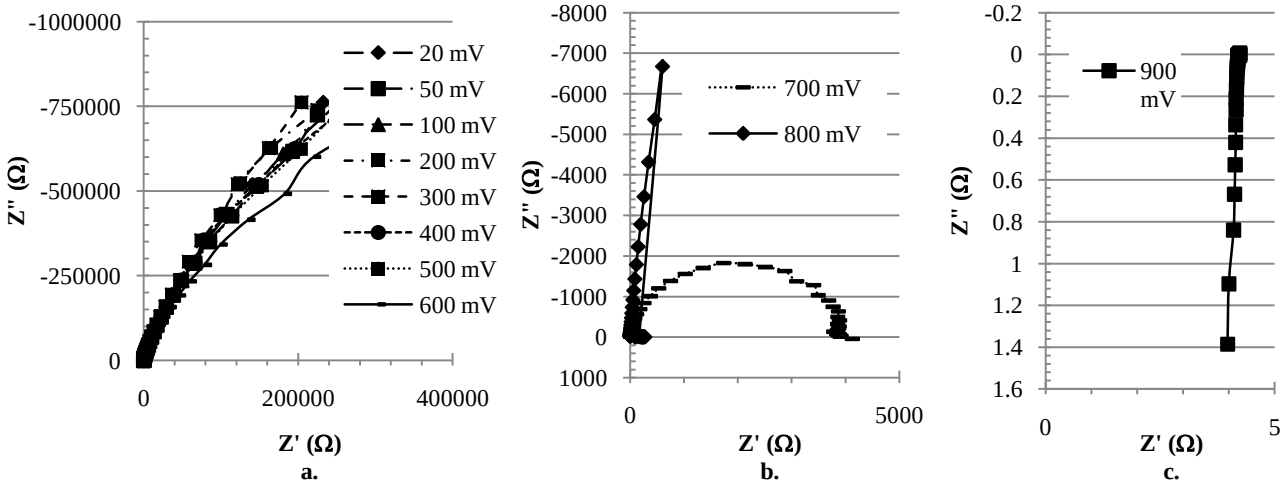

Figure 6 a, b and c. Effect of voltage amplitude on impedance - breakdown voltage.

This type of behaviour was repeated for a number of different film thicknesses and showed that there was typically a breakdown voltage beyond which the capacitor-like behaviour of the film broke down. Furthermore, once the film had broken down in this way (i.e. exceeded 900mV) the capacitor-like behaviour was destroyed and could not be recovered by reducing the voltage again, indicating that this change was permanent.

Using a value for breakdown voltage of 800 mV and a film thickness of 20 nm, it can be deduced that the field strength in the 40 MV/m. In other tests, similar values were found for the field strength in a film at the time of breakdown. Literature values of the dielectric breakdown strength of alumina are typically around 10 MV/m. As a result, it can be deduced that the breakdown voltage measured in these tests is causing breakdown of the dielectric properties of the film and once broken down, the dielectric properties of the film are not easily recovered. This also illustrates why past studies of impedance of native oxide films have not always been successful. Unless very small voltage amplitudes are used with a zero bias, it is quite possible to destroy these thin films simply by dielectric breakdown. It may also explain why the native oxide films tested soon after the samples were polished could not be measured. They were simply too thin and the dielectric properties were destroyed even at very low voltage amplitudes. In the experimental setup used here, it was not possible to get sensible results at voltage amplitudes below 2 mV. Whilst the dielectric properties of the films could be destroyed, it is not clear that this has led to accelerated wetting of the aluminium by the mercury. The observations in this paper suggest that wetting does not take place after dielectric breakdown and in fact the mercury droplet remains separated from the aluminium. This is the subject of further investigation.

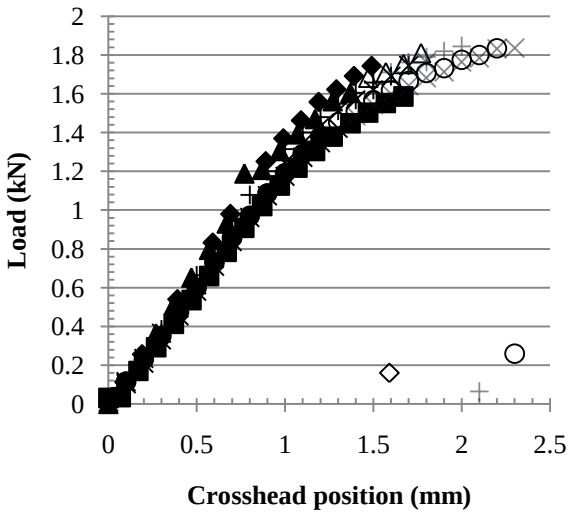

Figure 7 Effect of load on the onset of embrittlement. The unfilled or shadowed points represent conditions where the film had broken down.

3.3 Effect of load

In the literature of liquid metal embrittlement, it is generally accepted that embrittlement does not occur unless the material yields first. In this series of experiments, strips of 5083 were polished and loaded in 3 point bending with liquid mercury on the surface. The results of the testing are as shown in Figure 7. This figure shows the load points at which impedance measurements of the films were taken. The points that are either un-filled or shadowed represent the points at which no film was detected. That is, there was a short circuit between the mercury and the aluminium. From the figure, it can be seen that although many specimens failed as soon as the film broke down, a number of samples required considerable deformation after the film had short-circuited in order to cause failure. This suggests that it is not sufficient only for the film to short circuit in order for embrittlement to occur. Furthermore, it appears that in these experiments, the film short circuited at a roller position of 1.2 to 1.7. This corresponds approximately to the onset of plastic deformation.

4. CONCLUSIONS

This paper outlines a number of studies into the effects of mercury on the oxide film on 5083 aluminium alloy. It was found that the oxide film at the interface could be measured using impedance spectroscopy techniques and the film could be modelled effectively using the R-C-R circuit shown in Figure 1. However, the circuit was not stable and significant changes, particularly in R_p, were observed over time. Due to the thin nature of the oxide film, relatively small alternative voltages can cause field strengths in excess of the dielectric field strength of alumina and hence lead to film breakdown. Finally, it was found that plastic strain just beyond yield could cause the film to short circuit, although this would not necessarily lead to failure of sample by embrittlement.

5. REFERENCES

1. Bell, R.N., *Understanding and Preventing Failure of Aluminum Equipment in the Presence of Liquid Mercury*, in *Spring Meeting of the American Institute of Chemical Engineers*. 2005, AIChE: Atlanta, GA.
2. Bingham, M.D., *Field detection and implications of mercury in natural gas.* SPE Production Engineering, 1990. **5**(2): p. 120-124.
3. Coade, R. and D. Coldham, *The interaction of mercury and aluminium in heat exchangers in a natural gas plants.* International Journal of Pressure Vessels and Piping, 2006. **83**(5): p. 336-342.
4. Nelson, D.R., *Mercury attack of brazed aluminum heat exchangers in cryogenic gas service*, in *73rd Annual GPA Convention*. 1994: New Orleans, Louisiana. p. 178-183.
5. Wilhelm, S.M., *Risk Analysis for Operation of Aluminium Heat Exchangers Contaminated by Mercury.* Process Safety Progress, 2008. **28**(3): p. 259-266.
6. Wilhelm, S.M. and N. Bloom, *Mercury in petroleum.* Fuel Processing Technology, 2000. **63**: p. 1-27.
7. Wilhelm, S.M., *Design mercury removal systems for liquid hydrocarbons.* Hydrocarbon Processing 1999. **78**(4): p. 61-62.
8. Burstein, G.T. and R.J. Cinderey, *Evolution of the corrosion potential of repassivating aluminium surfaces.* Corrosion Science, 1992. **33**(3): p. 475-492.

9. Burstein, G.T. and R.M. Organ, *Repassivation and pitting of freshly generated aluminium surfaces in acidic nitrate solution.* Corrosion Science, 2005. **47**(12): p. 2932-2955.
10. Liu, Y., G.Z. Meng, and Y.F. Cheng, *Electronic structure and pitting behavior of 3003 aluminum alloy passivated under various conditions.* Electrochimica Acta, 2009. **54**(17): p. 4155-4163.
11. Vetter, K.J., *General kinetics of passive layers on metals.* Electrochimica Acta, 1971. **16**(11): p. 1923-1937.
12. McIntyre, D.R. and J.W. Oldfield, *Environmental attack of ethylene plant alloys by mercury*, in *Corrosion Prevention in the Process Industries*. 1988, NACE: Amsterdam. p. 239-252.
13. Hirschorn, B., et al., *Determination of effective capacitance and film thickness from constant-phase-element parameters.* Electrochimica Acta, 2009.

6. AUTHOR DETAILS

Richard Clegg is Director of the Process Engineering and Light Metals Centre at CQUniversity in Gladstone, a position he has held since 2007. He is a metallurgist who specialises in failure mechanisms in process plant equipment and is Editor in Chief of the journal *Engineering Failure Analysis*.

Ashutosh Srivastava has just completed his Masters from Stanford University in the US and is now joining Intel Corporation. Amoghavarsha M has recently completed a degree at NITK in India and will commence a DPhil at Oxford University this year. Both Ashutosh and Amoghavarsha were intern students with Prof.Clegg in Gladstone when this work was done.